Shape Evolution for Rigid and Nonrigid Shape Registration and Recovery

Junyan Wang and Kap Luk Chan
School of Electrical & Electronic Engineering
Nanyang Technological University
Singapore
{wa0009an,eklchan}@ntu.edu.sg

Abstract

This paper addresses the problem of rigid and nonrigid shape registration and recovery in the presence of shape deformation, missing parts and/or overlapping of multiple shapes. A novel shape evolution approach based on truncated warping transformation formulated in an Energy-Minimization-Curve-Evolution framework is proposed to solve this problem. We deterministically model the rigid and nonrigid shape deformation/registration as curve evolution by a warping function mapping. We also derive the curve evolution equation of warping to minimize functional energies. Hence, by selecting a prior shape as the initial curve for the curve evolution, the shape evolution for registration is within the shape space generated by the warping transformation of the prior shape. Based on the Fourier shape contour spectrum, local shape contour distortions that result in significant visual impact is considered to be largely contained in the changes of the high frequency components. Thus, the smoothing of the warping function by truncation is performed to recover the true shape. We adopted the Chan-Vese model and a truncated warping function to obtain our algorithm for shape registration and recovery. Experiments validated our model and algorithm quantitatively.

1. Introduction

Shape registration is often referred as the matching of points on a shape contour to such points on one or several reference shape(s)[10] [9] [8]. A shape may be distorted due to shape deformation, missing parts and/or overlapping of multiple shapes. Many existing methods cannot deal with the concurrent occurrence of these causes and recover the original or a deformed version of the shape. In this paper, we extend the scope of shape registration such that, given some reference shapes and a shape to be registered which may be a deformed version of one of the reference shapes, and possibly with distortions due to missing parts and/or overlapping of multiple shapes, shape registration is the process of finding a transformation of the deformation and recovering the true shape. Two examples of the registration problem are illustrated in Figures 1 and 2. Figure 3 illustrates a possible shape registration process, where the deformed and overlapped shape is registered and recovered to be the deformed prototype shape.

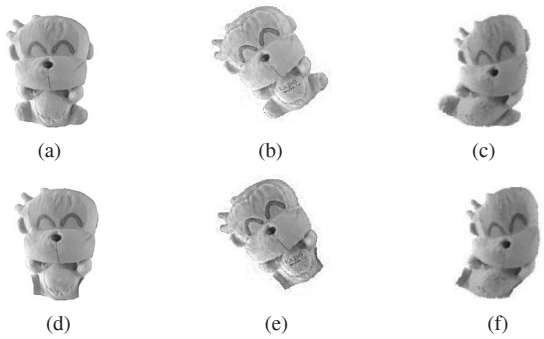

Figure 1: (a) The ground-truth of a monkey; (b) Rigidly transformed ground-truth of monkey; (c) Nonrigidly transformed ground-truth of monkey; (d) Monkey with missing parts; (e) Rigidly transformed monkey with missing parts; (f) Nonrigidly transformed monkey with missing parts.

In recent years, shape priors have been used in curve evolution frameworks for object segmentation and shape recovery [4] [11] [5] [6] [7] [13]. The idea is to restrict the active contours to evolve in a prior shape space by shape prior regularization. The corresponding curve evolution produces a closed curve through minimizing a functional energy within the prior shape space. The algorithms can therefore force the computed shape to follow a shape in the prior shape space. We notice that although shape prior driven curve evolution methods are developed for object segmentation, they implicitly accomplish shape registration. In what follows, we discuss some of the pioneering works which motivate our work.

Chen *et al*. [4] proposed a variational curve evolution

978-1-4244-3991-1/09/$25.00 ©2009 IEEE

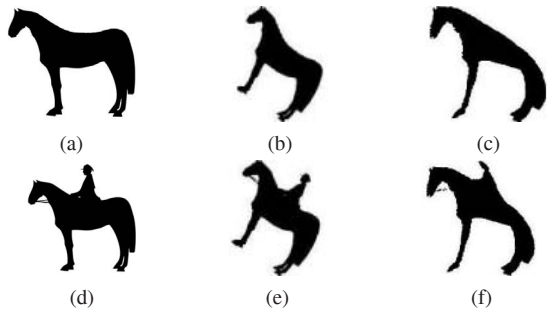

Figure 2: (a) The ground-truth of a horse; (b) Rigidly transformed ground-truth of horse; (c) Nonrigidly transformed ground-truth of horse; (d) Horse merged with rider; (e) Rigidly transformed horse merged with rider; (f) Nonrigidly transformed horse merged with rider.

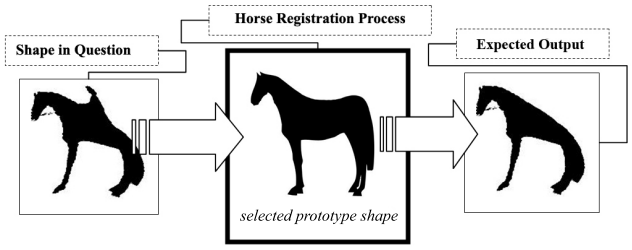

Figure 3: A horse registration process

framework for object segmentation by aligning the evolving curve with a reference shape. In the context of shape registration, this work only considered the rigid deformation. Nonrigid shape deformations were modeled ***statistically*** in [11] [5] [6] [7]. Leventon *et al*. [11] modeled shape variation using Principal Component Analysis (PCA), and measured the shape distance from a mean shape. Cremers *et al*. [5] [6] developed a framework involving both variational rigid shape alignment and statistical models. More recently, Etyngier *et al*. [7] formulated the space of prior shapes for curve evolution to be a shape manifold. However, the state-of-the-art statistical methodology for nonrigid shape prior modeling involves collecting many samples. This is because the dimensions of such shape representations are generally very high. It is also a problem to reduce the dimensions of the shape representation if there are insufficient learning samples. Furthermore, the prior shape are iteratively reproduced by projection to the prior shape space during the curve evolution, and this incurs extra computation.

Shape warping [1] [10] [8], which is essentially a closed-form point transformation, is a direct ***deterministic model*** for shape deformation. It has been used for registering shapes, and it is sometimes referred as deformable template matching. Comparing with recent shape prior based curve evolution approaches, there are three advantages of shape warping based registration: First, it can naturally handle nonrigid and rigid shape registration; Second, the number of reference shape samples to use can be as few as one and it is called a prototype; Third, there are no projections during the registration process. However, the registration process was generally based on a maximum *a posteriori* (MAP) estimation with a stochastic optimization process in which a global optimal solution or a good local optimal solution is sought at the cost of substantial computation. Yet, a deterministic gradient descent algorithm, as in the Energy-Minimization-Curve-Evolution framework, is preferred for the sake of efficiency. However, the curve evolution equation of warping for minimizing general functionals has yet to be derived. Besides, the former warping based registrations is not suitable for shape distortion due to missing parts or overlapping of multiple shapes because such registration methods are trying to match all the points on the reference shape contour to all the points on the contour of shapes to be registered.

The above motivates us to develop a warping based method for both shape registration and recovery in an Energy-Minimization-Curve-Evolution framework. Our approach can be summarized as follows.

1. We model the rigid and nonrigid registration process as a curve evolution driven by a closed-form warping. The corresponding vector field of the warping transformation is called *prior variation*.

2. We derive the curve evolution equation with the prior variation, and we call it the *prior variation curve evolution equation*. The technique that we developed for obtaining the curve evolution equation is named as *Calculus of Prior Variation*. Hence a warping based registration is realized by a deterministic gradient descent in an Energy-Minimization-Curve-Evolution framework. This gives rise to a shape evolution approach to registration and shape recovery.

3. Based on the Fourier shape contour spectrum, we consider that the shape distortion resulting in significant visual impact can be found in the changes of the high frequency components. Hence, we smooth the warping function by truncation to recover the shape while registering.

4. We adopt the Chan-Vese model [3] for the variational framework.

From our point of view, the contribution of this piece of work can be summarized as follows.

- The proposed method enables us to register a rigid or nonrigid shape in the presence, including concurrent presence, of shape deformation, missing parts and

merging of multiple shapes, with one selected prototype prior shape. The need for a large collection of samples for training the statistical shape prior models is avoided;

- The shape evolves within a prior shape space defined by the warping transformation and a prototype shape. Hence, no projections to the prior shape space are needed, and the final converged shape can be a deformed version of the prior shape. This is in contrast to the statistical shape prior driven curve evolution in which the curve is forced to follow the prior shape;
- We present a model of shape distortion of significant visual impact by using Fourier analysis.
- Furthermore, the curve evolution approach provides an alternative to the Monte Carlo scheme used in some other warping based registration or deformable template matching methods.

Our approach differs from that in [2] in that, only one prototype shape is used as the prior while in [2] the intensity or color information from additional images are used as priors for the registration and segmentation. Besides, our developed prior variation curve evolution can be used for minimizing arbitrary energy functional, while in [2], the curve evolution was only shown to be able to minimize a particularly formulated functional.

The rest of this paper is organized as follows. In section 2, we present the derivation of the prior variation curve evolution equation. In section 3 we incorporate the prior variation curve evolution equation of rigid and nonrigid warping transformation into the Chan-Vese model to obtain an active contour algorithm for shape registration and recovery. We evaluated our algorithm qualitatively and quantitatively in section 4 to validate our model and algorithm. Finally we conclude the paper in section 5.

2. Theoretical formulations

In this section, we derive the prior variation curve evolution equation. We also present our shape contour model that leads to the truncated warping function for shape registration and recovery.

2.1. Prior variation curve evolution due to warping transformation

To develop a warping based method for both shape registration and recovery in an Energy-Minimization-Curve-Evolution framework, we model the shape registration as a curve evolution represented by $C(p,t) = \vec{x}(p,t) = [x_1(p,t), x_2(p,t)]^T$, $\vec{x}(p,t) \in C \subset R^2$, where p is the parametrization and t is the artificial time of the evolution. $C(p,0) = C_0$ is the prototype prior shape. We then model the deformation of the points $\vec{x}$ on the curve C as a closed-form transformation by $\vec{f}$ with parameter θ that changes w.r.t. time as follows.

$$\vec{x}(p,t) = \vec{f}(\vec{x}(p,0), \theta(t)), \text{and } \theta(0) = 0 \tag{1}$$

If the function $\vec{f}$ is differentiable w.r.t. θ and θ is continuous w.r.t. t, we have that

$$\left.\frac{\partial \vec{f}(\vec{x}(p,0),\theta(t))}{\partial \theta}\right|_{\theta(t)=\theta(t_0)} = \left.\frac{\partial \vec{f}(\vec{x}(p,t_0),\theta(t))}{\partial \theta}\right|_{\theta(t)=0} \tag{2}$$

Thus, the curve evolution equation of Eq.(1) can be written as follows.

$$\frac{\partial C(p,t)}{\partial t} = \frac{\partial \vec{x}(p,t)}{\partial t} = \frac{d\theta}{dt}\frac{\partial \vec{f}(\vec{x}(p,0),\theta(t))}{\partial \theta} \tag{3}$$

By replacing $\vec{x}(p,0)$ with $\vec{x}(p,t)$, and following Eq. (2), we obtain,

$$\begin{aligned}\frac{\partial C(p,t)}{\partial t} &= \frac{d\theta}{dt}\left.\frac{\partial \vec{f}(\vec{x}(p,t),\theta(t))}{\partial \theta}\right|_{\theta(t)=0} \\ &= \frac{d\theta}{dt}\vec{V}^{\theta}(\vec{x}(p,t))\end{aligned} \tag{4}$$

where

$$\vec{V}^{\theta}(\vec{x}(p,t)) = \left.\frac{\partial \vec{f}(\vec{x}(p,t),\theta(t))}{\partial \theta}\right|_{\theta(t)=0} \tag{5}$$

$\vec{V}^{\theta}(\vec{x}(p,t)) = \vec{V}^{\theta}(\vec{x})$ is defined as the *prior variation*.

An example of the prior variation is the vector field of Lie group action. For example, a rotation can be written as:

$$\vec{x}(p,t) = \begin{pmatrix} \cos(\theta(t)) & \sin(\theta(t)) \\ -\sin(\theta(t)) & \cos(\theta(t)) \end{pmatrix} \vec{x}(p,0) \tag{6}$$

It can be easily seen that Eqs.(2)-(4) all hold for the above transformation. However, we have to emphasize that the vector field of Lie group action is one special case of the prior variations which we will discuss in the following sections.

We now derive the curve evolution equations by the process of *Calculus of Prior Variations* for the minimization of functional energies.

Let us consider the functional energy minimization problem as follows.

$$C^* = \underset{C}{\operatorname{argmin}}\, J(C(p,t)) = J([x_1(p,t), x_2(p,t)]^T) \tag{7}$$

where J is the energy functional to be minimized.

By calculus of variations, we obtain the following,

$$\frac{\partial J(C)}{\partial t} = \left\langle \nabla J(C), \frac{\partial C}{\partial t} \right\rangle^* \tag{8}$$

where $\nabla J(C) = [\frac{\partial J([x_1,x_2]^T)}{\partial x_1}, \frac{\partial J([x_1,x_2]^T)}{\partial x_2}]^T$, $\langle , \rangle^*$ denotes the L^2 inner product of 2-D vector valued functions.

Substituting Eq.(4) into the above we have,

$$\begin{aligned}\frac{\partial J(C)}{\partial t} &= \left\langle \nabla J(C), \frac{d\theta}{dt}\frac{\partial \vec{f}(\vec{x}(p,t),\theta)}{\partial \theta}\bigg|_{\theta=0} \right\rangle^* \\ &= \left\langle \nabla J(C), \frac{\partial \vec{f}(\vec{x}(p,t),\theta)}{\partial \theta}\bigg|_{\theta=0} \right\rangle^* \frac{d\theta}{dt} \\ &= \left\langle \nabla J(C), \vec{V}^\theta(t) \right\rangle^* \frac{d\theta}{dt} = \frac{\partial J}{\partial \theta}\frac{d\theta}{dt}\end{aligned} \tag{9}$$

Hence, we can apply the gradient descent w.r.t. θ to arrive at the following.

$$\frac{d\theta}{dt} = -\frac{\partial J}{\partial \theta} = -\left\langle \nabla J(C), \vec{V}^\theta(\vec{x}) \right\rangle^* \tag{10}$$

where $\vec{V}^\theta(\vec{x}) = \vec{V}^\theta(\vec{x}(p,t))$. By back substituting the above to the curve evolution equation of Eq. (4), we obtain the following.

$$\frac{\partial C(p,t)}{\partial t} = -\left\langle \nabla J(C), \vec{V}^\theta(\vec{x}) \right\rangle^* \vec{V}^\theta(\vec{x}) \tag{11}$$

which is our *prior variation curve evolution equation*. Interestingly, the parameters for the warping transformation θ is implicitly expressed in the form of a partial differential equation. It is not always necessary to find θ when finding the transformation for deformation as the latter is also expressed as a partial differential equation.

For the convenience of implementation, we substitute the above to the level set curve evolution equation[12] to arrive at the following.

$$\begin{aligned}\frac{\partial \Phi}{\partial t} &= -\nabla\Phi \frac{\partial C(p,t)}{\partial t} \\ &= \langle \nabla\Phi(\vec{x}), \vec{V}^\theta(\vec{x}) \rangle \left\langle \nabla J(C), \vec{V}^\theta(\vec{x}) \right\rangle^*\end{aligned} \tag{12}$$

where $\langle , \rangle$ is an inner product for vectors, Φ is generally a signed distance function that can be defined as

$$\Phi(\vec{x}) = \begin{cases} d(\vec{x}, C), & \vec{x} \in C \\ 0 & \vec{x} \in \partial C \\ -d(\vec{x}, C) & \vec{x} \bar{\in} C \end{cases} \tag{13}$$

where d is the Euclidean distance from a point to the curve C

2.2. Truncation of warping function for registration and recovery

There are quite a number of warping transformations used in the literature of warping based point, shape, image registrations [1] [10] [8]. We define the warping function that we shall use as follows.

$$\vec{x}(p,t) = \vec{f}_{rg}(\vec{x}(p,0), \theta_{rg}(t)) + \vec{f}_{nrg}(\vec{x}(p,0), \theta_{nrg}(t)) \tag{14}$$

where the transformation consists of rigid part $\vec{f}_{rg}$ and nonrigid part $\vec{f}_{nrg}$ with transformation parameters $\theta_{rg}(t)$ and $\theta_{nrg}(t)$, respectively.

By considering the rigid part as the global transformation for global registration and the nonrigid part as the local deformation, we can carry out the rigid part first. If the rigid part is smooth enough, the truncation of warping is on the nonrigid part only.

The rigid part is defined by the following equation.

$$\begin{aligned}&\vec{x}(p,t) = \vec{f}_{rgd}(\vec{x}(p,0), \lambda(t), \alpha(t), a(t), b(t)) \\ &= \begin{pmatrix} \lambda(t)\cos(\alpha(t)) & \sin(\alpha(t)) \\ -\sin(\alpha(t)) & \lambda(t)\cos(\alpha(t)) \end{pmatrix} \vec{x}(p,0) + \begin{pmatrix} a(t) \\ b(t) \end{pmatrix}\end{aligned} \tag{15}$$

where λ, α, a, b are all parameters of the transformation, and the origin of the transformation is placed at the centroid of the evolving shape. Note that the rigid part is defined as a similarity transformation which is more general than the rigid transformation.

We now consider the Fourier expansion of the shape contours, and thus the *Fourier shape contour spectrum*. Given a shape $S(p) = [x_1^s(p), x_2^s(p)]^T$, where the shape contour is essentially represented by a 2-D mapping from p to points $[x_1^s(p), x_2^s(p)]^T$, it is possible to represent the shape contour by a linear combination of the Fourier bases or Fourier expansion, as follows.

$$[x_1^s(p), x_2^s(p)]^T = \sum_{k=0}^{K} [c_{1k}^s, c_{2k}^s]^T e_k(p) \tag{16}$$

where $span\{e_0, e_1, ...\}$ is the Fourier orthogonal system, $[c_{1k}^s, c_{2k}^s]^T, k = 0, 1, ..., K$ are the coefficients of the Fourier bases that constitute the shape contour spectrum. Note that this spectrum is different from the Fourier shape descriptor, but the geometrical interpretation can be analogous, i.e., the coefficients of lower order terms correspond to smooth changes along the contour while the coefficients of higher order terms correspond to sharp changes along the contour.

Now we make the following assumption.

Assumption 2.1 *The distortion of the shape having significant visual impact, due to missing parts or merging of shapes, leads to changes in the high frequency components of the shape contour spectrum.*

From the above assumption, if the registration transformation is smooth enough, the high frequency components

on the evolving shape will not change. Hence, the registered shape will never match the distorted shape where the high frequency components changes. Because of this, we can recover the true shape or a deformed version of the true shape. We also illustrate the above assumption in Figure 4 to facilitate the understanding of the principle. Although the mathematical interpretation of this phenomenon is attainable, we decide to only include the principle but not the mathematical derivations in this paper. Now we consider

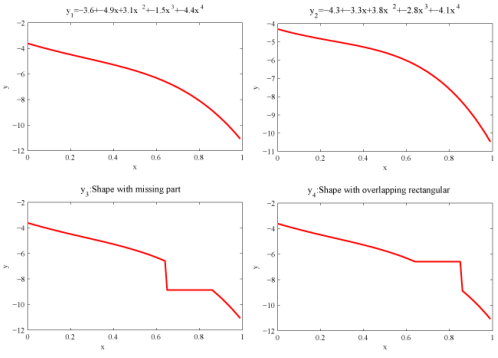

(a)

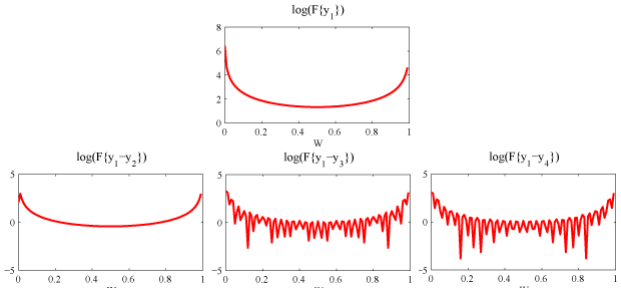

(b)

Figure 4: (a) upper left is an example of randomly generated polynomial y_1; upper right is the smoothly perturbed polynomial y_2 ; The bottom ones are y_1 with missing part y_3 and merging shape y_4. (b) The top shows the corresponding Fourier spectrum of y_1; The bottom line shows the shape differences w.r.t. y_1

the the following energy minimization for smoothing of the vector field of the warping function, $[v^1, v^2]^T$, which also achieves the smoothing of the warping transformation.

$$\begin{aligned} v^{i*}(s) &= \operatorname*{argmin}_{v^i} J(v^i), i = 1, 2 \\ \text{subject to: } &\int_C \|v^i - v^{i*}\|^2 ds \leq \varepsilon^2 \end{aligned} \tag{17}$$

where

$$J(v^i) = \int_C \|v^i\|^2 ds + \lambda \int_C \|\frac{dv^i}{ds}\|^2 ds \tag{18}$$

s is the parametrization by arc-length, λ is a user-defined regularization parameter, v^i is the observed vector field, ϵ is an prior upper bound of the distance from v^{i*} to v^i.

However, this corresponding solution requires us to iteratively parameterize the curve during the curve evolution. Hence we propose to minimize the following upper bound derived by a direct application of coarea formula and Cauchy-Schwarz inequality.

$$\begin{aligned} J^*(v^i) &= \int_\Omega \left(\|v^i\|^2 + \lambda \|\nabla v^i\|^2\right) \delta(\Phi) \|\nabla \Phi\| d\Omega \\ &\geq \int_C \|v^i\|^2 ds + \lambda \int_C \|\frac{dv^i}{ds}\|^2 ds \end{aligned} \tag{19}$$

where $\Phi = \Phi(\vec{x}, t)$ is a signed distance function defined by Eq. (13). By this, we avoid the parameterization of the curve, and thus $x(p, t)$ becomes $x(t) = \{\vec{x} | \Phi(\vec{x}, t) = 0\}$.

The corresponding Euler-Lagrange equation can be written as

$$\begin{aligned} \triangle v^i \delta(\Phi) &= -\frac{1}{\lambda} v^i \delta(\Phi) \\ \text{if, } &\int_\Omega \|v^i - v^{i*}\|^2 \delta(\Phi) d\Omega \leq \varepsilon^2 \end{aligned} \tag{20}$$

where Ω is the domain of the integral, $\triangle$ is the Laplace operator. Since $\delta(\Phi)$ since it is already in the level set implementation of curve evolution to extract v^i near $\Phi = 0$, we omit this in the following derivations.

We observe that Eq. (20) defines an eigenvalue problem for the Laplace operator, and the eigenfunctions of the Laplace operator for v^1, v^2 are the following orthogonal system defined on $[0, 1] \times [0, 1]$.

$$\begin{aligned} e^1_{mn}(x_1, x_2) &= 2 \sin(\pi n x_1) \cos(\pi m x_2) \\ e^2_{mn}(x_1, x_2) &= 2 \sin(\pi n x_2) \cos(\pi m x_1) \end{aligned} \tag{21}$$

Hence, the vector field of the warping transformation $[v^1, v^2]$ can be defined by a combination of the orthogonal functions as in Eq. (21). The corresponding transformation can be approximated by using the vector field near $t = 0$ as follows (also used in [1] [10] as the warping transformation).

$$\begin{aligned} \vec{x}(t) &= \vec{f}_{nrgd}\left(\vec{x}(0), \{\xi_{mn}, m, n = 1, 2, ...\}\right) \\ &= \vec{x}(0) + \sum_{m,n=1}^{\infty} \begin{pmatrix} \xi^1_{mn}(t) e^1_{mn}(x_1(0), x_2(0)) \\ \xi^2_{mn}(t) e^2_{mn}(x_1(0), x_2(0)) \end{pmatrix} \end{aligned} \tag{22}$$

where the coordinates are normalized to be within the $[0, 1] \times [0, 1]$ region, i.e., $\vec{x} = [x_1, x_2]^T \in [0, 1] \times [0, 1]$.

Finally, noting that there are higher order terms of the infinite series in Eq. (22) that correspond to the high frequency components, and hence we propose to truncate the infinite series by setting $1 \leq m + n \leq 3$ to ensure the warping to be sufficiently smooth.

3. Realization of the shape evolution

Instead of using a boundary-based active contour method, we propose to realize the rigid and nonrigid warping using the region based Chan-Vese active contour [3] with the prior variation based curve evolution and the truncated warping presented in the previous section.

3.1. Applying prior variation to Chan-Vese model

Following the Chan-Vese model, the corresponding curve evolution equation can be written as,

$$\begin{aligned} C_t &= -\nabla F(c_1, c_2, \Phi) \\ &= \left(\mu\kappa - v + \lambda_2|u_0 - c_2|^2 - \lambda_1|u_0 - c_1|^2\right)\vec{N} \\ &= G(C)\vec{N} \end{aligned} \quad \text{where,} \quad (23)$$

$$G(C) = \left(\mu\kappa - v + \lambda_2|u_0 - c_2|^2 - \lambda_1|u_0 - c_1|^2\right)$$

$$c_1 = \frac{\int_\Omega u_0 H(\Phi)d\Omega}{\int_\Omega H(\Phi)d\Omega}, \quad c_2 = \frac{\int_\Omega u_0(1 - H(\Phi))d\Omega}{\int_\Omega (1 - H(\Phi))d\Omega}$$

u_0 is the input image, $\mu, v, \lambda_1, \lambda_2$ are all parameters, κ is the curvature of the curve C, Φ is the signed distance function, H is a Heaviside function, $\vec{N} = -\frac{\nabla\Phi}{\|\nabla\Phi\|}$ is the outward normal of the curve. Note that Eq. (23) is not the original formulation of Chan-Vese active contours, but it can be derived by calculus of shape derivative of the Chan-Vese functional. By combining Eq. (23) with Eq. (12) we have

$$\Phi_t = \langle\nabla\Phi, \vec{V}^\theta\rangle \int\limits_{C=\{\vec{x}|\Phi=0\}} \langle\nabla F(c_1, c_2, \Phi), \vec{V}^\theta\rangle ds \quad (24)$$

And by applying the coarea formula, we have

$$\Phi_t = -\langle\nabla\Phi, \vec{V}^\theta\rangle \int_\Omega \delta(\Phi)G(C)\langle\frac{\nabla\Phi}{\|\nabla\Phi\|}, \vec{V}^\theta\rangle\|\nabla\Phi\|d\Omega \quad (25)$$

We shall drop the term $\|\nabla\Phi\|$ inside the integral for simplicity and thereafter, since $\|\nabla\Phi\| = 1$ in our case.

3.2. Rigid registration

For rigid registration by Eq. (15), the corresponding prior variations, with respect to different parameters, are as follows.

$$\begin{aligned} V^\lambda &= \left.\frac{\partial f}{\partial\lambda_1}\right|_{\lambda=0,\alpha=0,a=0,b=0} = \begin{pmatrix} x_1(0) \\ x_2(0) \end{pmatrix} \\ V^\alpha &= \left.\frac{\partial f}{\partial\alpha}\right|_{\lambda=0,\alpha=0,a=0,b=0} = \begin{pmatrix} x_2(0) \\ -x_1(0) \end{pmatrix} \\ V^a &= \left.\frac{\partial f}{\partial a}\right|_{\lambda=0,\alpha=0,a=0,b=0} = \begin{pmatrix} 1 \\ 0 \end{pmatrix} \\ V^b &= \left.\frac{\partial f}{\partial b}\right|_{\lambda=0,\alpha=0,a=0,b=0} = \begin{pmatrix} 0 \\ 1 \end{pmatrix} \end{aligned} \quad (26)$$

where we use $[x_1(0), x_2(0)]^T$ to represent the curve at the current time of shape evolution. Substituting the prior variations in Eq. (26) into Eq. (25), we obtain the level set curve evolution equations. Furthermore, we propose to use the joint level set curve evolution equation for all the 4 parameters as follows.

$$\Phi_t = -\sum_{\theta=\lambda,\alpha,a,b} \langle\nabla\Phi, \vec{V}^\theta\rangle \int_\Omega \delta(\Phi)G(C)\langle\frac{\nabla\Phi}{\|\nabla\Phi\|}, \vec{V}^\theta\rangle d\Omega \quad (27)$$

Note that the origin for the transformation is chosen to be the centroid of the evolving shape to facilitate the rotation and scaling.

3.3. Nonrigid registration

The nonlinear, or nonrigid prior variation corresponding to Eq. (22) can be written as follows.

$$\begin{aligned} V^{\xi^1_{mn}} &= \begin{pmatrix} 2\sin(\pi n x_1(0))\cos(\pi m x_2(0)) \\ 0 \end{pmatrix} \\ V^{\xi^2_{mn}} &= \begin{pmatrix} 0 \\ 2\sin(\pi n x_2(0))\cos(\pi m x_1(0)) \end{pmatrix} \end{aligned} \quad (28)$$

where we use $[x_1(0), x_2(0)]^T$ to represent the curve at the current time of shape evolution. Similarly, we can obtain the corresponding joint level set curve evolution equations for the above prior variations by substituting the above into Eq.(25).

$$\begin{aligned} \Phi_t = &-\sum_{n,m=1}^{N,M} \langle\nabla\Phi, \vec{V}^{\xi^1_{mn}}\rangle \int_\Omega \delta(\Phi)G(C)\langle\frac{\nabla\Phi}{\|\nabla\Phi\|}, \vec{V}^{\xi^1_{mn}}\rangle d\Omega \\ &-\sum_{n,m=1}^{N,M} \langle\nabla\Phi, \vec{V}^{\xi^2_{mn}}\rangle \int_\Omega \delta(\Phi)G(C)\langle\frac{\nabla\Phi}{\|\nabla\Phi\|}, \vec{V}^{\xi^2_{mn}}\rangle d\Omega \end{aligned} \quad (29)$$

where we set $1 \le m + n \le 3$. The coordinates are normalized to be within the $[0, 1] \times [0, 1]$ region.

4. Experimental results

In this section, we evaluate the proposed algorithm for shape registration and recovery. The experiments are designed with the following objectives in mind.

1. We evaluate our proposed algorithm for the registration of shape without missing parts or merging shapes by initializing a prototype shape.

2. We evaluate our proposed algorithm for shape registration in the presence of missing parts and/or merging shapes with only one prior shape.

3. We experimented with different rigid and nonrigid transformations.

We design an experiment to validate our theoretical formulations quantitatively. The size of the image for the monkey and the monkey with missing parts, the horse and the horse merged with the rider as shown in Figure 1 and Figure 2, is 128×128. We randomly generate the parameters for 50 rigid transformations, we also randomly generate the parameters for 50 truncated nonrigid warpings. Then we apply the corresponding rigid and nonrigid transformations to the monkey and horse shapes to obtain a total of 200 + 200 shapes for evaluation. The results of the experiments are shown in Figures 5 and 6, in which the abbreviations are summarized below:

Mon_R:rigidly transformed ground truth of monkey
Mon_R_MS:rigidly transformed monkey with missing parts
Mon_NR: nonrigidly transformed ground truth of monkey
Mon_NR_MS: nonrigidly transformed monkey with missing parts
Hor_R: rigidly transformed ground truth of horse
Hor_R_MG: rigidly transformed horse merged with rider
Hor_NR: nonrigdly transformed ground truth of horse
Hor_NR_MG: nonrigdly transformed horse merged with rider

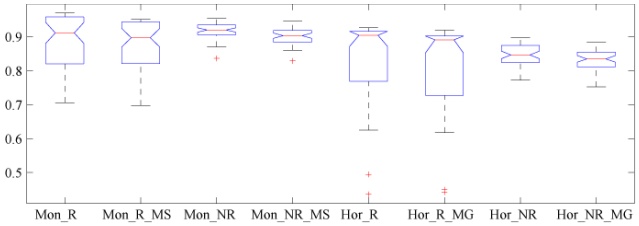

Figure 5: Shape Variation (vertical axis): the distances between the initial prototype shapes and the shapes to be registered. This is to show that the deformations of shapes is relatively large.

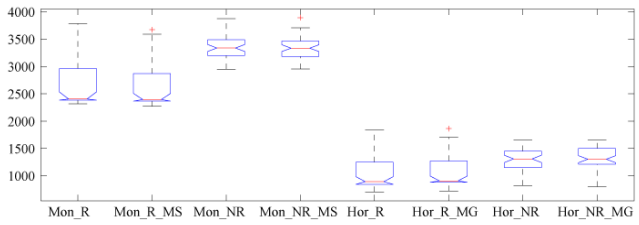

Figure 6: Registration performance measured by Jaccard's coefficients (vertical axis).

The probability density distributions that are used to generate random parameters are summarized in Table 1. For a better understanding of our algorithm, we also present some examples of the curve evolution in Figures 7, 8, 9 and 10. The statistical evaluations based on the Jaccard's coefficients are given by the box-plots in Figure 6. The top and bottom of each box are the 25th and 75th percentiles of the experimental results, respectively. The line in the middle of each box is the median. The registration performance as measured by the Jaccard's coefficients indicate the similarity between registration output and the deformed ground truths. Generally the registration performance based on the shape similarity measure is high. From Figures 5 and 6, we can also see that the differences between the initial prototype shapes and the shapes to be registered do not show any correlated effect on the performance of registration. This shows the insensitivity of the proposed algorithm to such differences. We also note that the Jaccard's similarity measure for the CVPR logo is 0.5385, but the result is visually acceptable. There is no quantitative results for the tattoo in Figure 10, as it is a real image without ground truth.

Transformations	Parameters	Distributions
Rigid, $\vec{x} \in [-1,1] \times [-1,1]$	θ	$U(-\pi/4, \pi/4)$
	λ	$U(-0.9, 1.1)$
	a,b	$U(-0.1, 0.1)$
Nonrigid, $\vec{x} \in [0,1] \times [0,1]$	ξ_{mn}^k, $1 \le m+n \le 3$, $k = 1,2$	$U(-0.125, 0.125)$

Table 1: The distributions of randomly generated parameters from uniform distributions

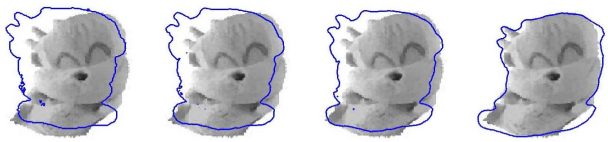

(a) (b) (c) (d)

Figure 7: Shape evolution for nonrigid registration of the monkey. The shapes are registered and recovered. (a) Initialization; (b) Iteration 20; (c) Iteration 40; (d) Convergence

(a) (b) (c) (d)

Figure 8: Shape evolution for nonrigid registration of the horse shape. The true shape is recovered. (a) Initialization; (b)Iteration 20; (c) Iteration 40; (d) Convergence

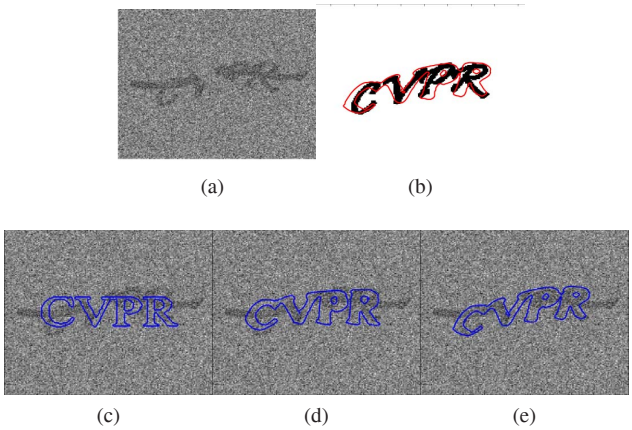

(a) (b) (c) (d) (e)

Figure 9: Registration for very noisy and severely distorted characters with both missing parts and overlapping shapes in (a); (b) Converged shape contour compared with ground-truth; (c) Initialization; (d) Iteration 150; (e) On convergence

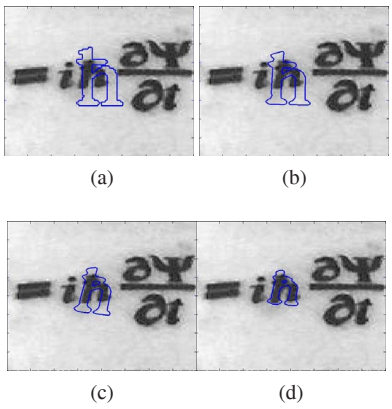

(a) (b) (c) (d)

Figure 10: Shape registration to find the "$\hbar$" in the tattoo on the skin. (a) Initialization; (b) Iteration 100; (c) Iteration 200; (d) Convergence

5. Conclusion

A novel shape evolution approach based on truncated warping transformation in an Energy-Minimization-Curve-Evolution framework is proposed for shape registration and recovery. The developed shape evolution algorithm can handle concurrent occurrence of shape deformation, missing parts and shape merges. Experiments show promising results.

References

[1] Y. Amit, U. Grenander, and M. Piccioni. Structural image restoration through deformable templates. *Journal of the American Statistical Association*, 86(414):376–387, 1991.

[2] L. Bertelli, M. Zuliani, and B. Manjunath. Pairwise similarities across images for multiple view rigid/non-rigid segmentation and registration. *Proceedings of the 11th IEEE International Conference on Computer Vision*, pages 1–8, Oct. 2007.

[3] T. Chan and L. Vese. Active contours without edges. *IEEE Transactions on Image Processing*, 10(2):266–277, Feb 2001.

[4] Y. Chen, H. D. Tagare, S. Thiruvenkadam, F. Huang, D. Wilson, K. S. Gopinath, R. W. Briggs, and E. A. Geiser. Using prior shapes in geometric active contours in a variational framework. *International Journal of Computer Vision*, 50(3):315–328, 2002.

[5] D. Cremers, T. Kohlberger, and C. Schnörr. Shape statistics in kernel space for variational image segmentation. *Pattern Recognition*, 36(9):1929–1943, 2003.

[6] D. Cremers, S. J. Osher, and S. Soatto. Kernel density estimation and intrinsic alignment for shape priors in level set segmentation. *International Journal of Computer Vision*, 3175:36–44, 2004.

[7] P. Etyngier, F. Segonne, and R. Keriven. Shape priors using manifold learning techniques. *Proceedings of the 11th IEEE International Conference on Computer Vision*, pages 1–8, Oct. 2007.

[8] C. A. Glasbey and K. V. Mardia. A review of image-warping methods. *Journal of Applied Statistics*, 25(2):155–171, April 1998.

[9] A. Jain, Y. Zhong, and M. Dubuisson Jolly. Deformable template models: A review. *Signal Processing*, 71(2):109–129, December 1998.

[10] A. Jain, Y. Zhong, and S. Lakshmanan. Object matching using deformable templates. *IEEE Transactions on Pattern Analysis and Machine Intelligence*, 18(3):267–278, Mar 1996.

[11] M. Leventon, W. Grimson, and O. Faugeras. Statistical shape influence in geodesic active contours. *Proceedings of the IEEE Conference on Computer Vision and Pattern Recognition*, 1:316–323 vol.1, 2000.

[12] S. Osher and J. A. Sethian. Fronts propagating with curvature-dependent speed: Algorithms based on hamilton-Jacobi formulations. *Journal of Computational Physics*, 79:12–49, 1988.

[13] M. Rousson and N. Paragios. Shape priors for level set representations. *Proceedings of the 7th European Conference on Computer Vision*, pages 78–92, 2002.